Exactly solvable models of irreversible adsorption with particle spreading

D. Boyer,[1] J. Talbot,[2] G. Tarjus,[1] P. Van Tassel,[1,3] and P. Viot[1]

[1]*Laboratoire Physique Théorique des Liquides, Université Pierre et Marie Curie, 4, place Jussieu,*
75252 Paris Cedex 05, France

[2]*School of Chemical Engineering, Purdue University, West Lafayette, Indiana 47907*

[3]*Centre Européen de Calcul Atomique et Moléculaire, Batiment 506, 91404 Orsay Cedex, France*

We introduce several models of irreversible adsorption in which nonrigid particles are deposited sequentially at random positions onto a line. Once adsorbed, a particle can immediately undergo an irreversible transition in which its size changes from 1 to $\sigma > 1$. In the first model, the center of mass of a particle remains unchanged during the spreading so that the transition occurs if there is enough room on both sides of the particle. In the second model, a particle grows if the total available space on both sides of the particle is larger than σ, irrespective of how it is distributed on the two sides; if the particle encounters its closest neighbor during the transition, it continues to spread on the unbounded side until it reaches a size σ. In the last model, the spreading transition is equivalent to a conformational change resulting from a tilting process; once adsorbed, the particle grows either to the right or to the left, provided that there is space available. We obtain expressions for the kinetics of these three models by introducing a gap density function. A comparison of results from each of these models allows us to determine the influence of the detailed mechanism of the spreading transition on the overall adsorption process.

I. INTRODUCTION

The physical adsorption of latexes [1,2], polyelectrolytes [3], and proteins [4–11] on solid surfaces is often a highly irreversible process in which surface diffusion and desorption play a minor role. Latexes can be well represented as rigid spherical objects, but some polymers [3] or proteins [4,6–8] may undergo, once adsorbed some structural or orientational changes due to the strong interaction with the substrate. Surface-induced conformational changes not only greatly decrease the tendency of proteins to desorb [6], but are also related to protein denaturation [6,8,11], a process which changes the tertiary structure and function of the adsorbed proteins.

As desorption is negligible and surface diffusion is very slow on the experimental time scale, the adsorption process evolves rapidly far from equilibrium and is essentially limited by geometrical exclusion effects between particles. Under these conditions, use of the random sequential adsorption (RSA) model, which takes into account both irreversibility and geometrical exclusion effects [12], is appropriate. In RSA, particles are deposited sequentially onto a surface. The position of a trial particle is chosen randomly, and the particle is adsorbed on the surface if it does not overlap previously adsorbed particles. If overlap occurs, it is rejected. In one dimension, this model is referred to as the "car parking problem" [13] and is exactly solvable.

The above discussion points to the desirability of extending the RSA model in order to include conformational and orientational changes of the particles on the surface [3]. As a first step in this direction, we introduce in this paper several solvable models which allow us to study qualitatively, but in great detail, the influence of

surface-induced conformational changes. In these models, the particles are deposited at a constant rate k per unit length like in an RSA process, but, in addition, they can instantly undergo an irreversible two-state transition on the surface. This transition represents, in a simplified way, a change of conformation (or orientation) of an adsorbed particle that is driven by a maximization of the area in contact with the substrate. We consider here the one-dimensional (1D) version of the problem, i.e., the deposition of rods on an infinite line. The diameter of the rods in solution is chosen as the unit of length. A configuration of adsorbed particles consists of a mixture of segments of sizes 1 and $\sigma > 1$, the latter corresponding to the final state of the structural transition on the surface.

Exclusion effects due to preadsorbed particles must be taken into account, not only for the insertion of a new particle, but also for the growth of a particle on the surface. In the first of the models we will consider, a particle spreads symmetrically from a size 1 to a size σ immediately following adsorption, given sufficient space on either side. Otherwise, its size remains equal to 1. In the second model, a particle again begins to grow symmetrically upon adsorption, but if it encounters its closest neighbor during the transition, it continues to spread on the unbounded side until it reaches a size σ (unless another neighbor prevents the full growth). Thus, the particle is prevented from spreading only if the interval in which it adsorbs is smaller than σ. In this model, particles can spread more easily and a larger saturation coverage is expected. The third model differs from the first in that the position of one of its ends is fixed during spreading. This model then mimics the adsorption process of elongated particles, which reach the surface "end on" and "tilt"

over if enough room is available either on the right or on the left. If space is available on both sides, the spreading direction is chosen randomly. This model is thus equivalent to an asymmetric spreading which occurs on one side or the other, but never both (unlike the second model). The three models are schematically depicted in Fig. 1.

For all models, we assume that the transition from size 1 to σ, if possible, occurs instantaneously following adsorption. In this limit, all the models can be solved exact-

ly. The next three sections are devoted to the derivation of the solutions to each of these models, and in the last section, their behavior is compared.

II. MODEL I: ADSORPTION WITH SYMMETRIC SPREADING

We introduce the gap distribution function $G(h,t)$, which is defined such that $G(h,t)dh$ represents the number density of gaps having a length between h and $h + dh$
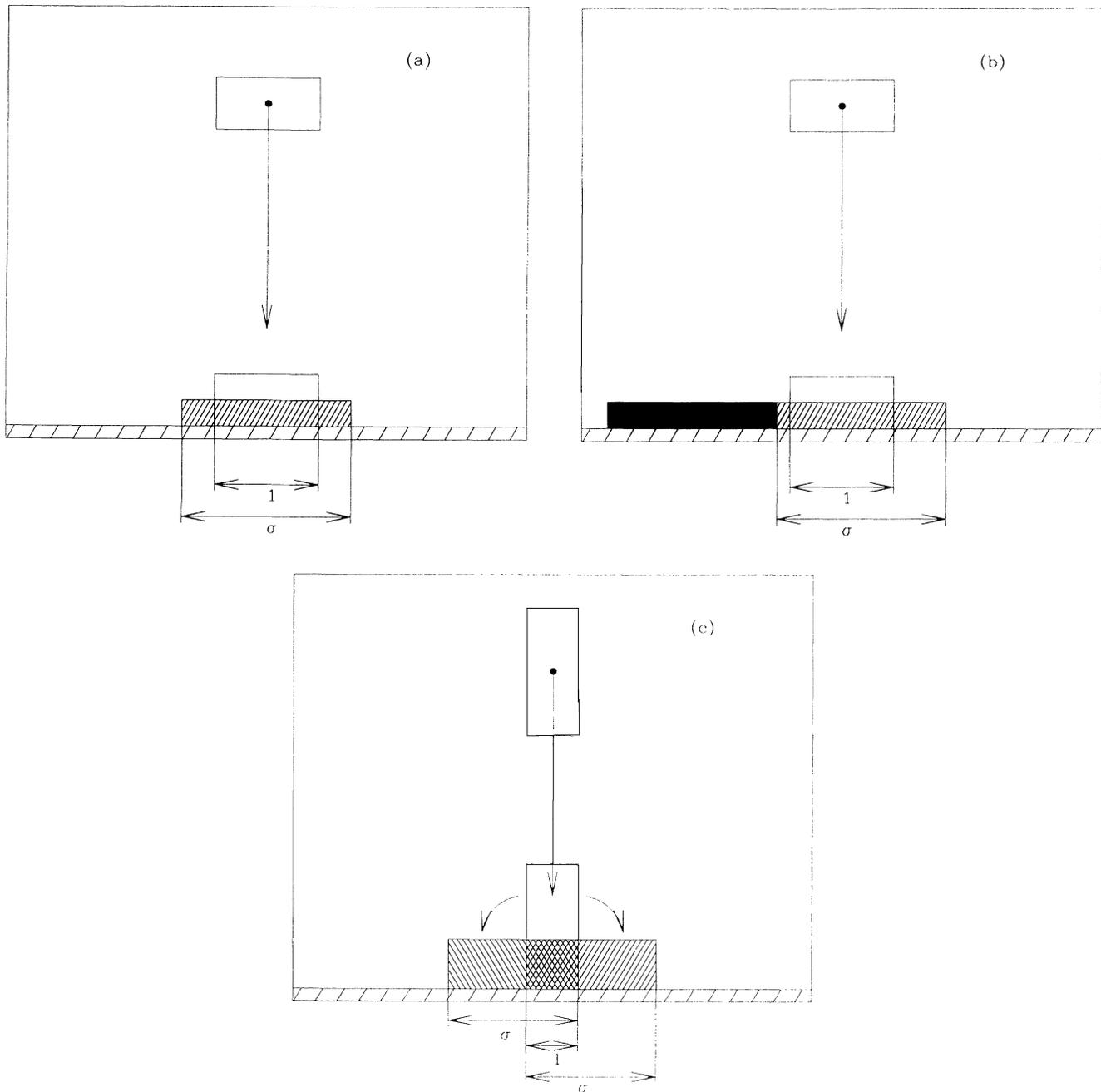
FIG. 1. Illustration of the deformation of a particle on the surface. We consider two states of the particle on the surface. (a) Model I: the particle is a rod of size 1 when it reaches the adsorbing line. If the neighbors are sufficiently far, the particle grows symmetrically. (b) Model II: growth can occur also close to a neighboring particle (black), but the particle spreading is asymmetric. (c) Model III: the particle adsorbs side on and tilts to the left or the right if space is available.

which are bounded by two particles of unspecified length (1 or σ). The rate equations of the gap distribution function can be written in a closed form by considering all the ways in which intervals may be created or destroyed during the deposition spreading process. For a given interval of length $h > \sigma$, the available length for the insertion of a particle of length 1 that eventually will stretch to a length σ is the inner interval of length $h - \sigma$, whereas the available length for the insertion of particles of length 1 that cannot undergo a transition is the sum of the right and left subintervals, each having length $(\sigma + 1)/2$. For an interval of length $\sigma > h > 1$, particles of length 1 can be in-

serted in the available length $h - 1$, but cannot expand. Conversely, an interval of length $h > (\sigma - 1)/2$ can be obtained by inserting either a particle of length 1 that stretches to a length σ on an interval of length $h' > h + \sigma$, or by inserting a particle of length 1 that cannot undergo a transition on an interval of length h' such that $h + (\sigma + 1)/2 > h' > 1 + h$. Finally, an interval of length $h < (\sigma - 1)/2$ can be obtained by inserting either a particle with a final length σ in an interval of length $h' > h + \sigma$, or by inserting a particle of final length 1 in an interval of length $h' > h + 1$. From the above arguments, we obtain the following set of coupled equations:

$$\frac{\partial G(h,t)}{\partial t} = \begin{cases} -(h-1)G(h,t) + 2\int_{h+1}^{h+(1+\sigma)/2} dh' G(h',t) + 2\int_{h+\sigma}^{+\infty} dh' G(h',t) & \text{for } h > 1, \quad (1) \\ 2\int_{h+1}^{h+(1+\sigma)/2} dh' G(h',t) + 2\int_{h+\sigma}^{+\infty} dh' G(h',t) & \text{for } 1 > h > (\sigma-1)/2, \quad (2) \\ 2\int_{h+1}^{+\infty} dh' G(h',t) + 2\int_{h+\sigma}^{+\infty} dh' G(h',t) & \text{for } (\sigma-1)/2 > h > 0, \quad (3) \end{cases}$$

where, without loss of generality, we have set the rate of adsorption per unit length to unity. The factor of 2 in the creation terms of the right-hand side of the preceding equations reflects the two possibilities of breaking a larger interval by inserting a particle. Equations (1)–(3) correspond to the case of a moderate deformation of the particles ($\sigma \leq 3$) [3]. The process for $\sigma > 3$ can also be described using the same method, but its solution, which requires successive iterations, will not be given here for the sake of simplicity. The solution of the above equations can be obtained by considering first the intervals larger than 1. Inserting the following ansatz,

$$G(h,t) = F(t)\exp(-(h-1)t) \quad \text{for } h > 1, \quad (4)$$

in Eq. (1) gives

$$\frac{dF(t)}{dt} = 2\frac{F(t)}{t}e^{-t}(e^{-(\sigma-1)t} - e^{-[(\sigma-1)/2]t} + 1), \quad (5)$$

the solution of which is

$$F(t) = t^2 \exp\left[-2\int_0^t dt' \left[\frac{1-e^{-\sigma t'}}{t'} - \frac{e^{-t'} - e^{-[(\sigma+1)/2]t'}}{t'}\right]\right]. \quad (6)$$

Introducing the exponential-integral function $E_1(x) = \int_x^{+\infty} \exp(-t)/t$, the function $F(t)$ can be rewritten as

$$F(t) = \left[\frac{\sigma+1}{2\sigma}\right]^2 \exp\left[-2\left[\gamma + E_1(\sigma t) - E_1\left[\frac{\sigma+1}{2}t\right]\right.\right.$$
$$\left.\left. + E_1(t)\right]\right], \quad (7)$$

where $\gamma = 0.577\cdots$ is the Euler constant. Once $G(h,t)$ is known for $h > 1$, one finds by integrating Eqs. (2) and (3)

$$G(h,t) = 2\int_0^t dt' \frac{F(t')}{t'}[1 - e^{[(\sigma-1)/2]t'} + e^{-(\sigma-1)t'}]e^{-ht'}$$
$$\text{for } 1 > h > (\sigma-1)/2, \quad (8)$$

and

$$G(h,t) = 2\int_0^t dt' \frac{F(t')}{t'}[1 + e^{-(\sigma-1)t'}]e^{-ht'}$$
$$\text{for } (\sigma-1)/2 > h > 0. \quad (9)$$

The gap distribution function has a finite discontinuity at the point $(\sigma - 1)/2$, which is due to the influence of the spreading transition on the creation of gaps of this length [see Eqs. (2) and (3)]. At the end of the process, $G(h, \infty)$ is discontinuous at $h = 1$ because there are no intervals larger than 1 [$G(h, \infty) = 0$ for $h > 1$], whereas also the intervals of length $h < 1$ cannot be destroyed (Fig. 2). Moreover, as in conventional RSA, $G(h, \infty) \sim -\ln(h)$ when $h \rightarrow 0$. A similar logarithmic divergence is expected in higher dimensions.

From the gap distribution function, it is possible to obtain the number density $\rho_1(t)$ of particles of length 1 and
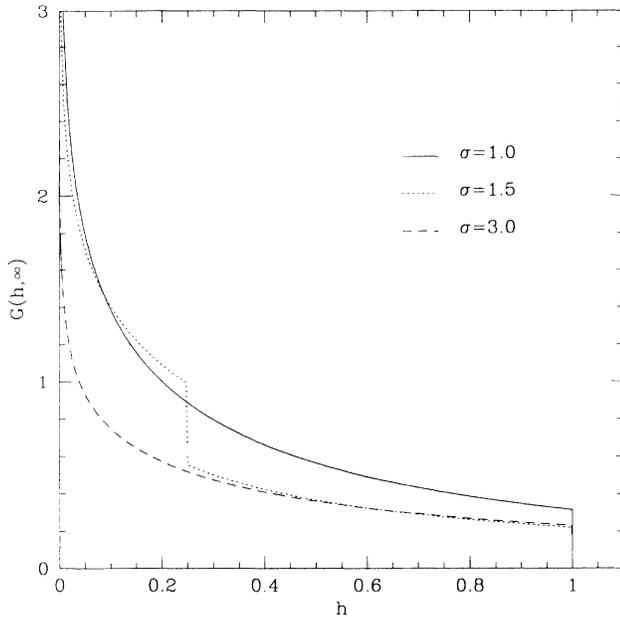
FIG. 2. Model I: gap distribution function $G(h, \infty)$ vs h for $\sigma = 1, 1.5, 3.0$ at the jamming limit. Note the finite discontinuities at the points $h = (\sigma - 1)/2$ and $h = 1$, and the logarithmic divergence when $h \rightarrow 0$.

the number density $\rho_\sigma(t)$ of particles of length σ. The kinetic equations satisfied by these two quantities can be written as

$$\frac{d\rho_i(t)}{dt} = \Phi_i(t), \quad i = 1, \sigma , \tag{10}$$

where $\Phi_i(t)$, the probability of adding one more particle of final size i, is equal to the fraction of line that is available for particles i. Since, for a given interval of length $h > 1$, the available length for inserting a particle that remains of length 1 is equal to $\sigma - 1$ if $h > \sigma$ or $h - 1$ for $1 < h < \sigma$, the function $\Phi_1(t)$ is equal to

$$\Phi_1(t) = \int_1^{+\infty} dh \, (\min(\sigma, h) - 1) G(h, t) . \tag{11}$$

The insertion of particles of final length σ is only possible for intervals larger than σ, and the function $\Phi_\sigma(t)$ is thus given by

$$\Phi_\sigma(t) = \int_\sigma^{+\infty} dh \, (h - \sigma) G(h, t) . \tag{12}$$

Inserting Eq. (4) in Eqs. (11) and (12) and using Eq. (10) leads to the following expressions for the number densities $\rho_1(t)$ and $\rho_\sigma(t)$:

$$\rho_1(t) = \int_0^t dt' \frac{F(t')}{t'^2} (1 - e^{-(\sigma - 1)t'}) , \tag{13}$$

and

$$\rho_\sigma(t) = \int_0^t dt' \frac{F(t')}{t'^2} e^{-(\sigma - 1)t'} . \tag{14}$$

At short times, $\rho_\sigma(t) = t + O(t^2)$ and $\rho_1(t) = [(\sigma$

$-1)/2] t^2 + O(t^3)$. The latter expression results from the fact that a particle of final size 1 can appear only if its spreading is prevented. This is only possible when a first particle has been already adsorbed.

The covered fraction of line, which we denote $\theta(t)$ as in the two-dimensional system, and the total number density $\rho(t)$, are obtained from Eqs. (13) and (14) by linear combinations,

$$\theta(t) = \rho_1(t) + \sigma \rho_\sigma(t) , \tag{15}$$

$$\rho(t) = \rho_1(t) + \rho_\sigma(t) , \tag{16}$$

and one may easily check that they indeed satisfy the sum rules, $\theta(t) = 1 - \int_0^\infty dh \, hG(h, t)$ and $\rho(t) = \int_0^\infty dh \, G(h, t)$.

Close to the jamming limit, $\rho_\sigma(t)$ approaches its saturation value exponentially:

$$\rho_\sigma(\infty) - \rho_\sigma(t) \sim \left[\frac{\sigma + 1}{2\sigma} \right]^2 e^{-2\gamma} \frac{e^{-(\sigma - 1)t}}{t^2} . \tag{17}$$

The largest particles do not contribute significantly near the end of the filling process since most intervals become smaller than σ. The particles that are adsorbed in the asymptotic regime are thus prevented from growing, which results in the following algebraic law:

$$\rho_1(\infty) - \rho_1(t) \sim \rho(\infty) - \rho(t) \sim \left[\frac{\sigma + 1}{2\sigma} \right]^2 \frac{e^{-2\gamma}}{t} . \tag{18}$$

The asymptotic behavior of $\rho(t)$ and $\theta(t)$ is thus similar to that of a simple RSA process.

Figure 3 compares the time evolution of the partial and total coverages $\rho_1(t)$, $\rho_\sigma(t)$, and $\theta(t)$ for different values of the size σ. At short times, the filling is essentially due to
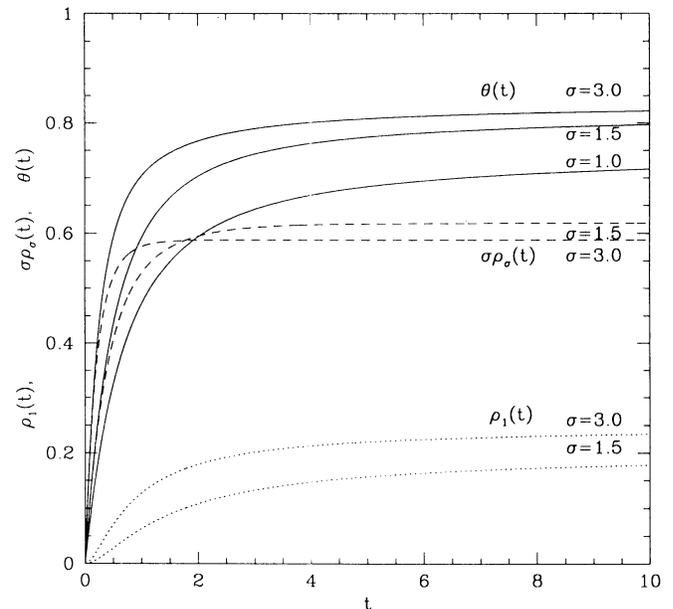
FIG. 3. Model I: time dependence of the total covered fraction of line $\theta(t)$, the fraction covered by particles of size 1, $\rho_1(t)$, and $\sigma \rho_\sigma(t)$, which is covered by particles of size σ, for $\sigma = 1.0, 1.5, 3.0$.
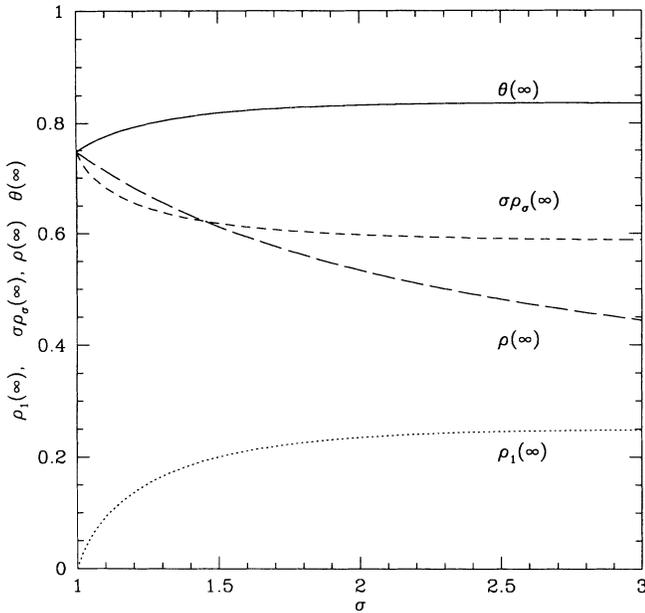
FIG. 4. Model I: σ dependence of the saturation densities, $\rho_1(\infty)$ and $\rho(\infty)$, and partial and total coverages, $\sigma\rho_\sigma(\infty)$ and $\theta(\infty)$.

the particles which can grow $[\rho_\sigma(t) \sim \theta(t)]$, but, for long times, the adsorption proceeds with practically no spreading $[\rho_1(\infty) - \rho_1(t) \sim \rho(\infty) - \rho(t)]$. At short times, the partial coverage of largest particles is more efficient if the size is larger, but their corresponding saturation den-

sities are lower.

Figure 4 displays the σ dependence of the partial and total saturation coverages, $\rho_1(\infty)$, $\sigma\rho_\sigma(\infty)$, $\theta(\infty)$, as well as that of the total density $\rho(\infty)$. The saturation coverages have a relatively weak dependence on the final size σ. But the partial densities, $\rho_1(\infty)$ and $\rho_\sigma(\infty)$, change rapidly around $\sigma = 1$. A close examination of Eq. (13) and Eq. (14) reveals a nonanalytic behavior,

$$\rho_1(\infty) \simeq \rho_\sigma(\infty) - \rho_{\sigma=1}(\infty)$$

$$\sim -e^{-2\gamma}(\sigma - 1)\ln(\sigma - 1) + O(\sigma - 1) . \quad (19)$$

III. MODEL II: ADSORPTION WITH ASYMMETRIC SPREADING

To solve the second model, we again focus on the gap distribution function $G(h,t)$. For a given interval of length $h > \sigma$, the available length for the insertion of particles of final length σ is the inner interval of length $h - 1$: in this model, if a particle lands in a space of length σ, it is able to grow. For intervals of length $\sigma > h > 1$, only particles of final length 1 can be inserted in the available length $h - 1$. Similarly, an interval of length $h > (\sigma - 1)$ can be obtained by inserting a particle of final length σ in an interval of length $h' > \sigma$. Finally, an interval of length $h < (\sigma - 1)$ can be obtained by inserting either a particle of final length σ in an interval of length $h' > \sigma$, or by inserting a particle of final length 1 in an interval of length $\sigma > h' > 1$. From the above arguments, the following set of coupled equations can be derived. For $\sigma \leq 2$, one obtains

$$\frac{\partial G(h,t)}{\partial t} = \begin{cases} -(h-1)G(h,t) + 2\int_{h+\sigma}^{+\infty}dh'G(h',t) + (\sigma-1)G(h+\sigma,t) & \text{for } h > 1 , & (20) \\[2mm] 2\int_{h+\sigma}^{+\infty}dh'G(h',t) + (\sigma-1)G(h+\sigma,t) & \text{for } 1 > h > (\sigma-1) , & (21) \\[2mm] 2\int_{h+1}^{\sigma}dh'G(h',t) + 2\int_{h+\sigma}^{+\infty}dh'G(h',t) + (\sigma-1)G(h+\sigma,t) & \text{for } (\sigma-1) > h > 0 . & (22) \end{cases}$$

As in the symmetric model I, this asymmetric model can be solved for $\sigma > 2$, which implies slight modifications in the above equations. However, we restrict ourselves here to the case of moderate spreading.

The rate equations may be solved by inserting the ansatz of Eq. (4) in Eq. (20). The function $F(t)$ obeys

$$\frac{dF(t)}{dt} = F(t)e^{-\sigma t}\left[\frac{2}{t} + (\sigma - 1)\right] , \quad (23)$$

which gives

$$F(t) = t^2\exp\left[-2\int_0^t dt'\frac{1-e^{-\sigma t'}}{t'} + \frac{\sigma-1}{\sigma}(1-e^{-\sigma t})\right]$$

$$= \sigma^{-2}\exp\left[-2[\gamma + E_1(\sigma t)] + \frac{\sigma-1}{\sigma}(1-e^{-\sigma t})\right] , \quad (24)$$

where $E_1(t)$ is the exponential-integral function. By integrating Eq. (21) and (22), one obtains the full solution for the gap distribution function $G(h,t)$:

$$G(h,t) = \begin{cases} \int_0^t dt' F(t') e^{-(\sigma-1)t'} ((\sigma-1) + \dfrac{2}{t'}) e^{-ht'} & \text{for } 1 > h > (\sigma-1), \quad (25) \\ \\ 2\int_0^t dt' \dfrac{F(t')}{t'} [e^{-ht'} - e^{-(\sigma-1)t'}] + \int_0^t dt' F(t') e^{-(\sigma-1)t'} \left[(\sigma-1) + \dfrac{2}{t'} \right] e^{-ht'} & \text{for } (\sigma-1) > h > 0. \quad (26) \end{cases}$$

Contrary to model I, the gap distribution function $G(h,t)$ is now a piecewise continuous function, but $(\partial G(h,t)/\partial h)$ has a finite discontinuity at $h = \sigma - 1$. At the jamming limit, $G(h,\infty)$ is discontinuous at $h = 1$ (Fig. 5). Also, at the jamming limit, $G(h,\infty)$ does not diverge as $-\ln(h)$ when $h \to 0$. Instead, $G(h,t)$ has a finite value at contact. Another importance difference is that the spreading mechanism leads to cluster formation. Therefore, in addition to the regular gap distribution $G(h,t)$, there exists a singular contribution $G_s(t)\delta(h)$, which represents the density of particle contacts and whose time evolution is governed by

$$\frac{dG_s(t)}{dt} = (\sigma-1) \int_\sigma^{+\infty} dh \, G(h,t) . \quad (27)$$

After insertion of Eq. (4), one obtains

$$G_s(t) = (\sigma-1) \frac{F(t)}{t} e^{-(\sigma-1)t} . \quad (28)$$

To derive expressions for the number densities $\rho_1(t)$ and $\rho_\sigma(t)$, we again start with Eq. (10). Since, for a given interval of length $h > 1$, the available length for inserting a particle of final length 1 is equal to $h - 1$ for $h < \sigma$ and
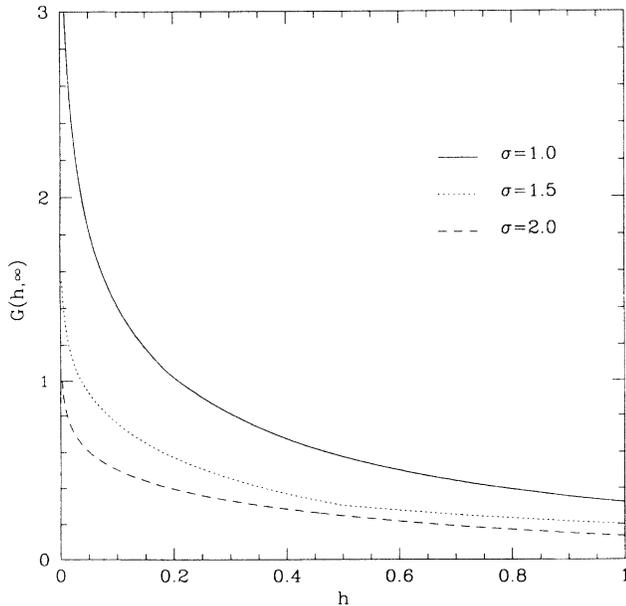
FIG. 5. Model II: regular part of the gap distribution function $G(h,\infty)$ vs h for $\sigma = 1, 1.5, 2.0$ at the jamming limit. Note the small cusp at the point $h = (\sigma-1)/2$.

0 for $h > \sigma$, the function $\Phi_1(t)$ is given by

$$\Phi_1(t) = \int_1^\sigma dh \, (h-1) G(h,t) . \quad (29)$$

The addition of particles of final length σ is only possible for intervals larger than σ, but the available length is that in which a particle of initial size 1 can adsorb, i.e., $h - 1$. The function $\Phi_\sigma(t)$ is then equal to

$$\Phi_\sigma(t) = \int_\sigma^{+\infty} dh \, (h-1) G(h,t) . \quad (30)$$

Introducing Eq. (26) in Eqs. (29) and (30) and using Eq. (10) yields

$$\rho_1(t) = \int_0^t dt' \frac{F(t')}{t'^2}$$
$$- \int_0^t dt' \frac{F(t')}{t'} e^{-(\sigma-1)t'} \left[(\sigma-1) + \frac{1}{t'} \right] \quad (31)$$

and

$$\rho_\sigma(t) = \int_0^t dt' \frac{F(t')}{t'} e^{-(\sigma-1)t'} \left[(\sigma-1) + \frac{1}{t'} \right] . \quad (32)$$

At short times, $\rho_\sigma(t) = t + O(t^2)$ and $\rho_1(t) = [(\sigma-1)^2/6] t^3 + O(t^4)$. The latter can be interpreted by noting that an adsorbed particle remains at size 1 only when it is inserted in an interval of length smaller than σ. This condition requires that at least two particles have already adsorbed.

The asymptotic approach towards the jamming limit is described by

$$\rho_1(\infty) - \rho_1(t) \sim \left[\frac{e^{-\gamma}}{\sigma} \right]^2 \frac{e^{[(\sigma-1)/\sigma]}}{t} , \quad (33)$$

and

$$\rho_\sigma(\infty) - \rho_\sigma(t) \sim (\sigma-1) \left[\frac{e^{-\gamma}}{\sigma} \right]^2 e^{[(\sigma-1)/\sigma]} \frac{e^{-(\sigma-1)t}}{t} . \quad (34)$$

The asymptotic kinetics are thus essentially the same for model II as for model I. Note, however, the $1/t$ dependence in Eq. (34) in place of $1/t^2$ in Eq. (17). The late stage of the filling process is dominated by the insertion of particles of size 1 that have no space to stretch on the line. The approach to saturation for the particles which grow on the surface is fast (essentially exponential).

In Fig. 6, we display the time dependence of $\rho_1(t)$, $\rho_\sigma(t)$, $\theta(t)$, and $\rho(t)$ for various values of σ. The partial
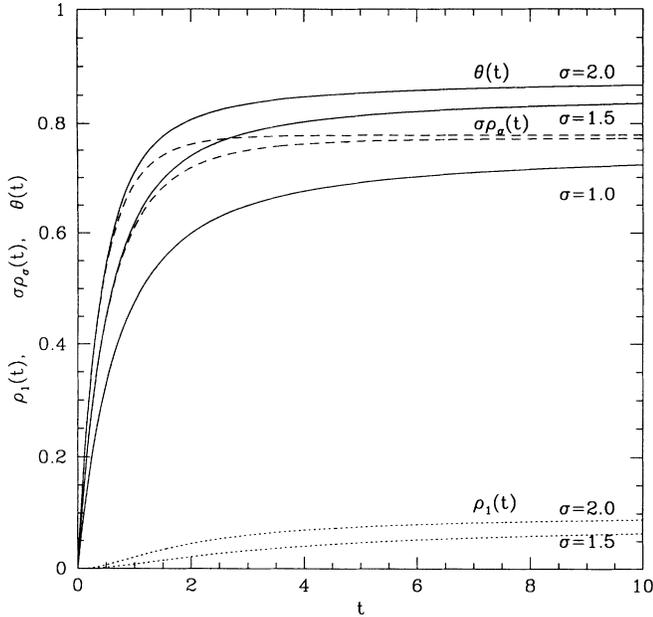
FIG. 6. Model II: time dependence of the total fraction of covered line $\theta(t)$, the fraction covered by particles of size 1, $\rho_1(t)$, and $\sigma\rho_\sigma(t)$, which is covered by particles of size σ, for $\sigma = 1.0, 1.5, 2.0$.

FIG. 7. Model II: σ dependence of the saturation densities, $\rho_1(\infty)$ and $\rho(\infty)$, and partial and total coverages, $\sigma\rho_\sigma(\infty)$ and $\theta(\infty)$.

and total saturation coverages and the total saturation density are plotted in Fig. 7. Note that, contrary to model I, even $\sigma\rho_\sigma(\infty)$ increase with σ. This reflects the higher efficiency of the spreading mechanism in model II.

It is worth noting that in this model the addition of particles of final size σ is independent of the presence of particles of final size 1. The reason is that a particle of size 1 can only occupy a gap of length less than σ, which is in any case unavailable for large particles. Moreover, the adsorption-spreading process for the σ particles is *exactly* equivalent to a generalized ballistic deposition model in which σ particles can adsorb on the line either by direct deposition or after "rolling" over a preadsorbed particle [14]. The ratio of the rate of direct deposition versus the rate of rolling is equal to

$$a = \frac{(\sigma - 1)}{2\sigma} \ . \tag{35}$$

As in the generalized ballistic deposition model, σ particles form connected clusters and the cluster densities can be directly obtained from the solution given in Ref. 14. [See Eq. (32) of this reference, in which t should be replaced by σt and a by (35).] For instance, at the jamming
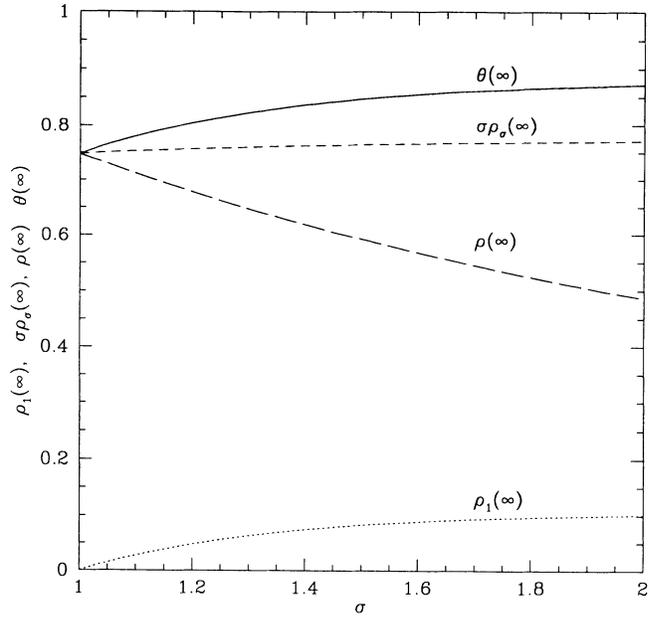
limit, the behavior of the density of clusters formed by s particles, $\rho_s(\infty)$, for asymptotically large clusters $(s \rightarrow +\infty)$ is given by

$$\rho_s(\infty) \sim \frac{(\sigma - 1)^{(s-1)}}{\sigma^s} \frac{1}{s!} \ . \tag{36}$$

The density of the clusters decreases very fast (faster than exponential) with their size. As noted by Evans and Nord [15], this seems to be a general feature of irreversible filling which does not allow for cluster-cluster coalescence.

IV. MODEL III: ADSORPTION WITH TILTING

For this model, examination of the time evolution of the gaps also leads to a set of closed equations for the distribution function $G(h, t)$. For a given interval of length $1 < h < \sigma$, only end-on (unspread) particles can be inserted. For $\sigma < h < (2\sigma - 1)$, the available length for particles which cannot spread, or tilt, is $(2\sigma - 1 - h)$, whereas the available length for particles which adsorb "side on" (i.e., spread) is equal to $2(h - \sigma)$. For larger intervals $(h > 2\sigma - 1)$, an adsorbed particle may always tilt. Thus, for $\sigma \leq 2$, the gap distribution function $G(h, t)$ evolves according to

$$\frac{\partial G(h,t)}{\partial t} = \begin{cases} -(h-1)G(h,t) + 3\int_{h+\sigma}^{h+2\sigma-1} dh' G(h',t) + 2\int_{h+2\sigma-1}^{+\infty} dh' G(h',t) & \text{for } h > 1 \ , & (37) \\ 3\int_{h+\sigma}^{h+2\sigma-1} dh' G(h',t) + 2\int_{h+2\sigma-1}^{+\infty} dh' G(h',t) & \text{for } 1 > h > \sigma-1 \ , & (38) \\ 4\int_{h+\sigma}^{h+2\sigma-1} dh' G(h',t) + 3\int_{h+2\sigma-1}^{+\infty} dh' G(h',t) + 2\int_{h+1}^{h+\sigma} dh' G(h',t) & \text{for } \sigma-1 > h > 0 \ . & (39) \end{cases}$$

The different factors in the creation terms of the right-hand side of the equations take into account all the ways of breaking a larger interval by inserting a particle which tilts either randomly (if a space is available on both sides), or only to the left or to the right (if a neighboring particle is nearby). The last right-hand term of Eq. (39) corresponds to the adsorption of particles which do not have space for tilting. A slightly different set of equations is obtained for $\sigma > 2$, but it will not be detailed here. Using the ansatz of Eq. (4), Eq. (37) can be solved by means of a function $F(t)$ which obeys

$$\frac{dF(t)}{dt} = \frac{F(t)}{t}(3e^{-\sigma t} - e^{-(2\sigma-1)t}),$$

(40)

and is thus given by

$$F(t) = \frac{2\sigma-1}{\sigma^3}\exp(-2\{\gamma + 3E_1(\sigma t) - E_1[(2\sigma-1)t]\}),$$

(41)

where $E_1(t)$ is the exponential-integral function. By integrating Eqs. (38) and (39), one obtains the full solution for the gap distribution function:

$$G(h,t) = \begin{cases} \int_0^t dt' \dfrac{F(t')}{t'}(3e^{-(\sigma-1)t'} - e^{-2(\sigma-1)t'})e^{-ht'} & \text{for } 1 > h > (\sigma-1), \quad (42) \\[2em] \int_0^t dt' \dfrac{F(t')}{t'}(2 + 2e^{-(\sigma-1)t'} - e^{-2(\sigma-1)t'})e^{-ht'} & \text{for } (\sigma-1) > h > 0. \quad (43) \end{cases}$$

In this model, $G(h,t)$ is discontinuous at $h = \sigma - 1$. At the jamming limit, $G(h,\infty)$ is also discontinuous at $h = 1$ and has a logarithmic divergence when $h \to 0+$ (see Fig. 8).

From arguments similar to those discussed above, the probability of adding one particle of final size 1 is

$$\Phi_1(t) = \int_1^\sigma dh\,(h-1)G(h,t) + \int_\sigma^{2\sigma-1} dh\,(2\sigma-1-h)G(h,t),$$

(44)

and the probability of adding one particle of final size σ is

$$\Phi_\sigma(t) = \int_\sigma^{2\sigma-1} dh\,2(h-\sigma)G(h,t) + \int_{2\sigma-1}^\infty dh\,(h-1)G(h,t).$$

(45)

By introducing Eq. (43) in Eqs. (44) and (30) and using Eq. (10), one may obtain the number densities

$$\rho_1(t) = \int_0^t dt' \frac{F(t')}{t'^2}[1 - e^{-(\sigma-1)t'}]^2,$$

(46)
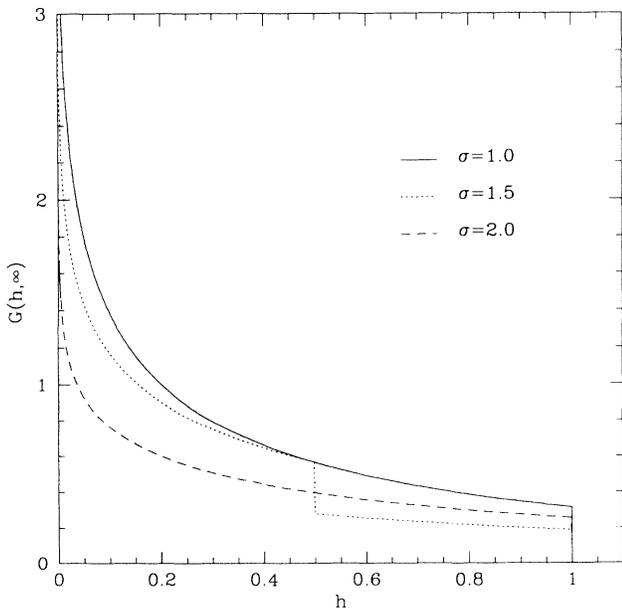
FIG. 8. Model III: gap distribution function $G(h,\infty)$ vs h for $\sigma = 1, 1.5, 2.0$ at the jamming limit. Note the finite discontinuities at the points $h = \sigma - 1$ and $h = 1$, and the logarithmic divergence when $h \to 0$.
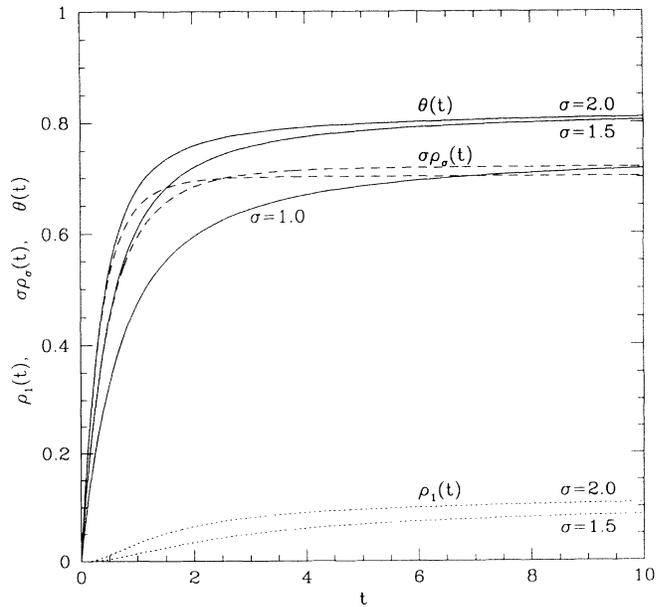
FIG. 9. Model III: time dependence of the total fraction of covered line $\theta(t)$, the fraction covered by particles of size 1, $\rho_1(t)$, and $\sigma\rho_\sigma(t)$, which is covered by particles of size σ, for $\sigma = 1.0, 1.5, 2.0$.
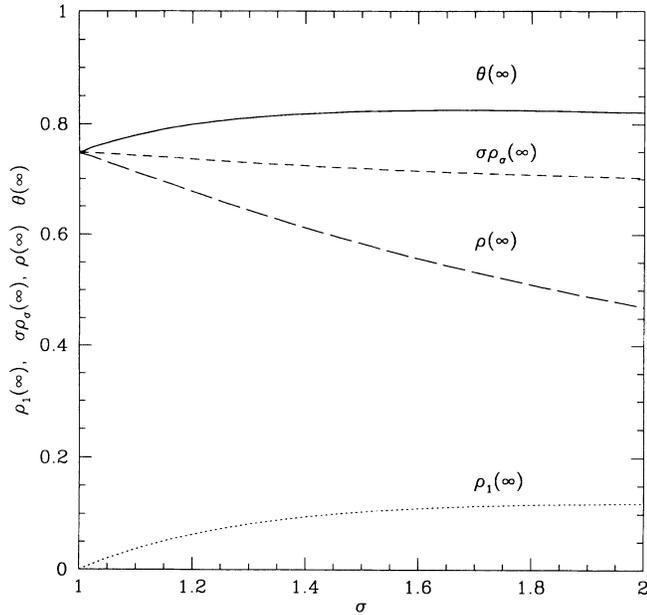
FIG. 10. Model III: σ dependence of the saturation densities, $\rho_1(\infty)$ and $\rho(\infty)$ and partial and total coverages, $\sigma\rho_\sigma(\infty)$ and $\theta(\infty)$.

$$\rho_\sigma(t)=\int_0^t dt' \frac{F(t')}{t'^2} e^{-(\sigma-1)t'}[2-e^{-(\sigma-1)t'}] \ . \qquad (47)$$

As in models I and II, the fractional coverage of the line $\theta(t)$ and the total number density $\rho(t)$ are obtained by combining Eqs. (46) and (47) and Eqs. (15) and (16) and the sum rules are obviously satisfied. The short time expansions of $\rho_1(t)$ and $\rho_\sigma(t)$ are the same as in model I, as are the asymptotic kinetics (up to trivial multiplying constants). The time evolution of the partial and total densities and coverages is illustrated in Fig. 9 and the σ dependence of their saturation values in Fig. 10.

V. DISCUSSION

The three models considered above have many similar features, like, e.g., the asymptotic kinetics and greater coverage compared to RSA without spreading. Model II differs in that it leads to cluster formation of large particles and represents a more efficient way of filling the space. In order to estimate the spreading effect during the adsorption process, the ratio $\theta(t)/\rho(t)$ can be interpreted as a mean size of adsorbed particles $\bar\sigma(t)$. Figure 11 compares the time evolution of $\bar\sigma(t)$ for the three models at two different sizes.

An interesting quantity is the partial coverage of the large particles $\sigma\rho_\sigma(\infty)$. It is reasonable to assume that in many experimental scenarios the particles of size 1 are more weakly bound to the substrate than the particles of size σ. These particles may be washed out by replacing the protein solution by a pure buffer solution, and $\sigma\rho_\sigma(\infty)$ could be experimentally determined [16]. It is

easy to show that the analytic solutions obtained for $\sigma \leq 3$ [Eq. (14), model I] or $\sigma \leq 2$ [Eq. (32), model II and Eq. (47), model III] are valid for the whole range of σ. In all cases, $\sigma\rho_\sigma(\infty)$ reaches an asymptotic value when $\sigma \to +\infty$ which is different from zero, and hence the number density $\rho_\sigma(\infty)$ goes to zero as $1/\sigma$. The σ dependence of $\sigma\rho_\sigma(\infty)$ is plotted in Fig. 12. For all models, $\sigma\rho_\sigma(\infty)$ rapidly reaches a plateau value when σ in-
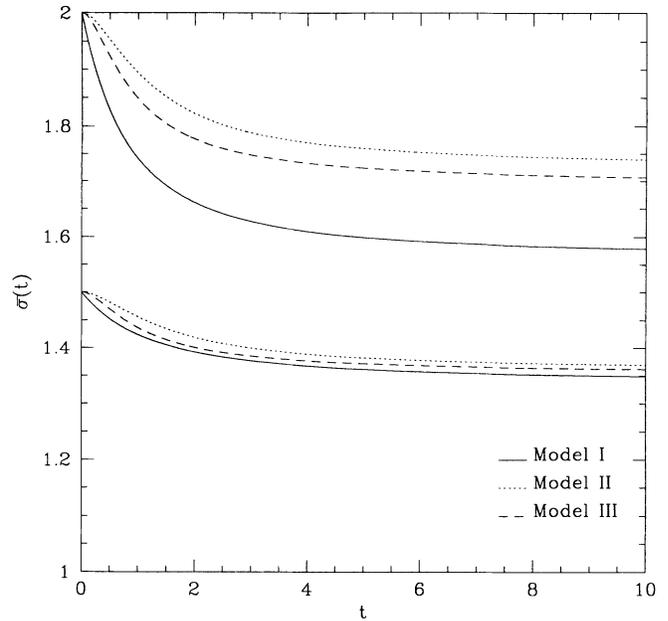
FIG. 11. Time evolution of mean size of adsorbed particles for the three models and for $\sigma=1.5,2.0$.
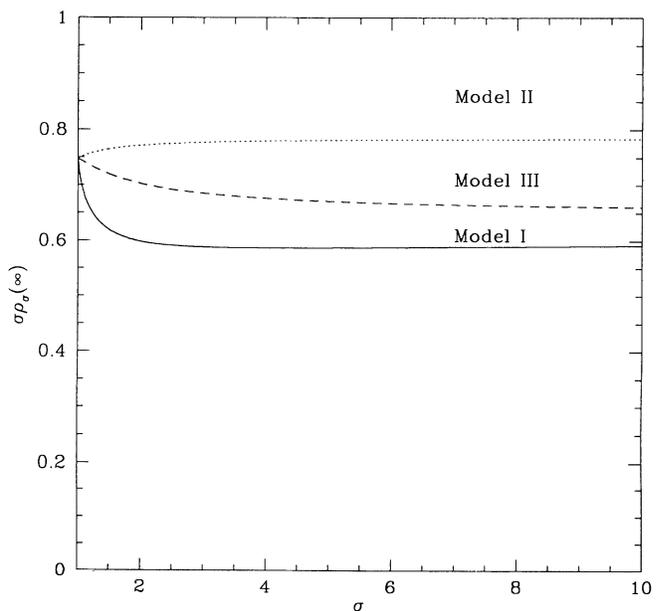
FIG. 12. Comparison of σ dependence of the coverage of the largest particles, $\sigma\rho_\sigma(\infty)$ for the three models.

creases. As expected, Model II leads to a highest fraction of line covered by largest particles.

In this paper, we have investigated three adsorption models in which particles undergo a conformational or structural change once adsorbed. Assuming that the transition is instantaneous, we are able to obtain solutions for these one-dimensional adsorption-spreading models with different spreading mechanisms, and hence analyze their influence on the overall adsorption process.

[1] G. Y. Onoda and E. G. Liniger, Phys. Rev. A **33**, 715 (1986).

[2] Z. Adamczyk, M. Zembala, B. Siwek, and P. Warszýnski, J. Colloid. Interface Sci. **140**, 123 (1990).

[3] A. Elaissari and E. Pefferkorn, J. Colloid. Interface Sci. **143**, 85 (1991).

[4] J. Feder, J. Theor. Biol. **87**, 237 (1980).

[5] J. Feder and I. Giaever, J. Colloid. Interface Sci. **78**, 144 (1980).

[6] J. D. Andrade and V. Hlady, Ann. N.Y. Acad. Sci. **516**, 158 (1987).

[7] M. E. Soderquist and A. G. Walton, J. Colloid. Interface Sci. **75**, 386 (1980).

[8] M. J. Mura-Galelli, J. C. Vogel, S. Behr, E. F. Bres, and P. Schaaf, Proc. Natl. Acad. Sci. **88**, 5557 (1991).

[9] P. Schaaf, Ph. Déjardin, A. Johner, and A. Schmitt, Langmuir **8**, 514 (1992).

[10] J. Ramsden, Phys. Rev. Lett. **71**, 295 (1993).

[11] R. Kurrat, J. Ramsden, and J. E. Prensil (unpublished).

[12] For a comprehensive review, see J. W. Evans, Rev. Mod. Phys. **65**, 4281 (1993).

[13] A. Rényi, Sel. Trans. Math. Stat. Prob. **4**, 205 (1963).

[14] P. Viot, G. Tarjus, and J. Talbot, Phys. Rev. E **48**, 480 (1993).

[15] J. W. Evans and R. S. Nord, Phys. Rev. A **31**, 3831 (1985).

[16] I. Lundström, Phys. Scr. **T4**, 5 (1983).